Wind Resistance Performance of Long-Span Steel Truss Bridges Across Gorges in Mountainous Areas

Kai Wang, Haili Liao and Jun Liu

Research Centre for Wind Engineering, Southwest Jiaotong University, Chengdu 610031, China
Corresponding author: Kai Wang, wangk1010@126.com

Abstract

This paper has carried out a comprehensive description on two long-span steel truss suspension bridges in China's western area, which includes the selection of design wind parameters, results of section model tests and process of optimizing the aerodynamic shape. The methods and results of selecting design wind parameters of the bridges in the mountainous valley are firstly introduced in the paper. Then the process and results of section model tests of the two bridges are presented. Next a series of optimization tests are conducted aiming at the wind-induced vibration of the main beam and analysis of all the optimization tests have been made to select the best measure for vibration suppression of the wind-resistance characteristics. It not only meets the need of bridge wind-resistance design, but also provides a reference for future design.

1 Introduction

Comprehensive studies have been conducted on wind-resistance performance of long-span steel truss bridges in plains and coastal areas. However for long span bridges especially with steel truss girder across gorges in mountainous areas, the wind-resistance performance are still in question. Comparing with wind in plain and coastal areas, the wind in the gorges is stronger, more frequent and high turbulent with prominent non-stationary characteristics. The spatial distribution of its wind velocity field is complex and has significant three-dimensional characteristics. The prediction and measurements of wind-induced vibration response in the gorges are obviously different from other areas. The special case is that the long-span steel truss bridges are always built between two peaks with the gorge area below the bridge which makes the condition more complex. The wind field is different not only between the middle of the bridge and both sides of the slopes, but also between the location of the bridge and the surroundings of the bridge. Because of the mountain topography, airflow may be wavy so that non-stationary characteristics of natural wind will have a very negative impact on the bridge structure. Lacking of observation materials and due to regulation limitations, if the design wind speed is obtained based on conventional method which are later used to do wind-resistance test, it might lead to unsafe results. Two long-span steel truss bridges, Baling River Bridge and Dimu River Bridge, which are constructed across gorges, are discussed in this paper to show the particularity of wind field in the mountainous areas and the likely occurrence of the wind-induced vibrations of long-span steel truss bridges. Measures to suppress the flutter of steel truss bridges are also presented.

Baling River Bridge and Dimu River Bridge are two large steel truss suspension bridges. Both two bridges cross big gorges that are steep on both sides with abrupt topographical changes and uneven terrain, the depths of which are all several hundred meters. The two bridges both located in the karst topographical area. Weather conditions, typical mountainous gorge wind, are similar at the bridge sites. Baling River Bridge is a steel truss suspension bridge with its main span 1088 meters. The width of the main beam is 28m and the height is 10 m (Figure 1). Dimu River Bridge is also a steel truss suspension bridge with its main span 538 m. The width of main beam is 27 m, which is composed of a steel beam with a height of 4.5 m and orthotropic plate with a height of 0.8 m (Figure 2). With long span, low self-vibration frequency, sensitivity to the wind qualities of both the two bridges, the flutter

stability becomes the key problem that is also typical in wind resistance and stability of the bridges under complex wind conditions in China's western mountainous areas. The dynamic characteristics of the two bridges are listed in Table 1.

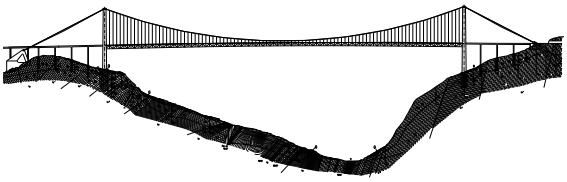

Figure 1 Arrangement of Baling River Bridge

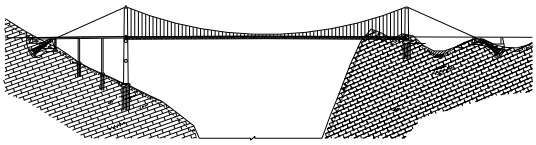

Figure 2 Arrangement of Dimu River Bridge

Table 1 Dynamic characteristics of the Two Bridges

Mode of vibration	Baling River Bridge	Dimu River Bridge
	Frequency /(hz)	Frequency /(hz)
The first symmetrical vertical bending	0.157	0.229
The first antisymmetry vertical bending	0.112	0.188
The first symmetric reverse	0.273	0.477
The first antisymmetry reverse	0.329	0.526

2 Wind Parameters at bridge site

Both bridges are located in the southwestern China, famous for its gorge topography. Both sides of the bridges are cliffs and steeps that are precipitous and complex. When natural wind flows though the gorge, it will be zoomed in or zoomed out, reversed or turned and then produces a number of vortices. All the above reasons make the wind field extremely complex. In order to determine the actual wind environment at the bridge site, taking Baling River Bridge as an example, the basic design wind of the bridge is determined as 24.9 m/s through in-situ measurement, numerous simulation (CFD) and topography tests at the bridge site.

According to Wind-resistant Design Specification for Highway Bridges, the maximum wind speed with recurrence period 100 years can be obtained using extreme value distribution Gumbel Type I and yearly extreme wind records of nearby metrological stations. The basic wind speed of Dimu River Bridge can be predicted as 26.92 m/s.

Since the bridge is located across a gorge, the determination of the design wind speed on the deck must take the gorge's complex terrain effects into consideration, by which the design wind speed will be modified. Assuming basic wind speed from gorge bridges virtual weather station is the inlet wind speed in the gorge, basic design wind speed of bridges built across gorges can be obtained from the following formula

$$u_{\mathrm{d}} = \left[\qquad\qquad\right] \tag{1}$$

In the formula, ud is basic design wind speed, u10 is basic wind speed from virtual weather station, H is the depth of the gorge, when a bridge is built across a gorge, H can be the height from the deck to the bottom of the gorge. B1 is the width of the gorge, it is usually the length of the bridge. B2 is the width of the bottom of the gorge, κ is gorge effect correction coefficient. From formula (1), design basic speed of Dimu River Bridge can be predicted as 34.80m/s.

Figure 3 Observation Tower at the Bridge Site

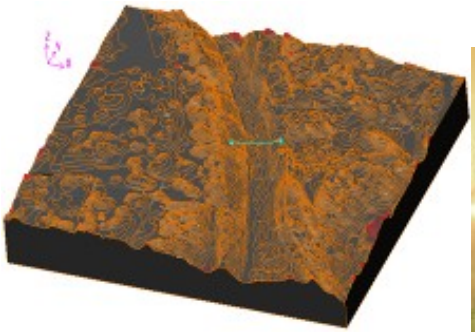

Figure 4 Calculation Area 3d View

Figure 5 Terrain Model in Wind Tunnel

3 Section Model Test

3.1 Static Loading

Static load coefficient is a non-dimensional coefficient that represents the magnitude of the force under the mean wind for the various structure sections and reflects aerostatic reaction of the bridge due to the wind. Now with the development of theory and computer technology, many people often use CFD software calculate the three component force coefficient for main beam. But for steel truss beam, there are obvious error between the results from CFD software and from actual. For truss beam, wind tunnel test is still required. In figure 6 and figure 7, there are steel truss beam cross section of Baling River Bridge and Dimu River Bridge.

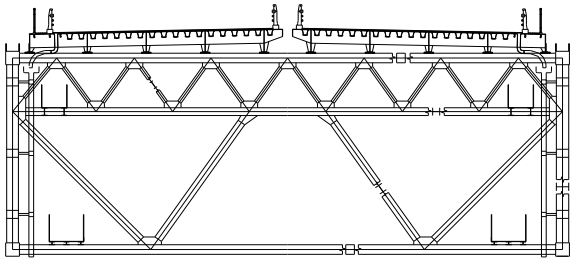

Figure 6 Main Beam Cross Section of Baling River Bridge

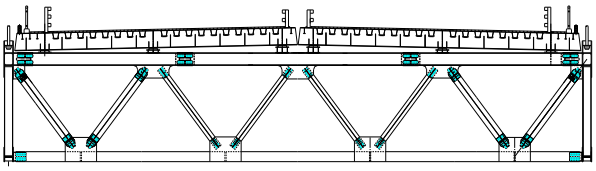

Figure 7 Main Beam Cross Section of Dimu River Bridge

There are two ways to express the effect on the main girder of the static force components by the coordinate system of the three different, as the body axis coordinate system (coordinate system along the section centroid axis) and the wind axis coordinate system (coordinate system along the direction of the wind). The static three component coordinate system is shown in figure 6. The three static force coefficients under the wind axis coordinate system Press the type definition:

$$\text{Resistance Coefficient:} \quad C_D(\alpha) = F_D(\alpha) \Big/ \left(\frac{1}{2}\rho v^2 HL\right)$$

$$\text{Lift Coefficient:} \quad C_L(\alpha) = F_L(\alpha) \Big/ \left(\frac{1}{2}\rho v^2 BL\right)$$

$$\text{Torque Coefficient:} \quad C_M(\alpha) = M_Z(\alpha) \Big/ \left(\frac{1}{2}\rho v^2 B^2 L\right)$$

Type: α is the flow angle of attack; $\frac{1}{2}\rho v^2$ is the air pressure; *H, B ,L* were the height, width, length; $F_D(\alpha)$, $F_L(\alpha)$, $M_Z(\alpha)$ were the resistance coefficient, lift coefficient, torque coefficient under the wind axis coordinate system. The resistance coefficient and lift coefficient could be got through change $F_D(\alpha)$ into $F_H(\alpha)$ and change $F_L(\alpha)$ into $F_V(\alpha)$, $M_Z(\alpha)$

and C_M 'α are the same under the two axis coordinate system, but resistance coefficient and lift coefficient need to coordinate conversion relations as shown in figure 8.

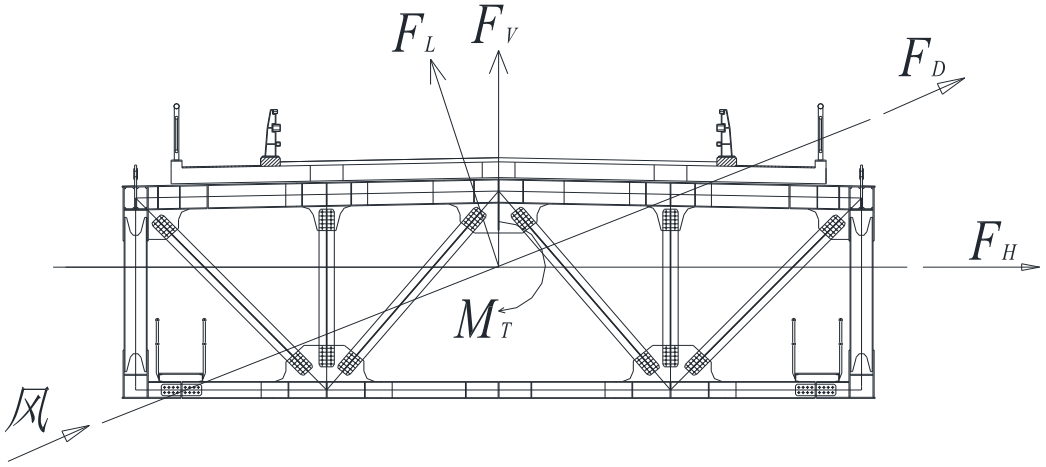

Figure 8 Schematic Plot of Body Axis Coordinate System and Wind Axis Coordinate System

For Baling River Bridge, the width of main beam is 28 m, the height is 10 m, the distance between each mode is 10.8 m. For the wind tunnel test of the main beam static section model, a geometrical scale of 1:47.5 with a 2.095 m in length is selected for section model. For Dimu River Bridge, its main span is 538 meters. The width of main beam is 27 meters, which is consisted of steel beam with the height of 4.5 meters and orthotropic plate with the height of 0.8 meter. A geometrical scale of 1:50 with a 2.095 m in length is selected for section model. Tests are carried out under uniform flow condition, the attack angle of the incoming flow is from -12° to 12°, the increment is 1°. Under the wind speed which is 15 m/s, the standard beams of Baling River Bridge and Dimu River Bridge in the completed state are tested. Testing results are shown in Figure 9 and Figure 10.

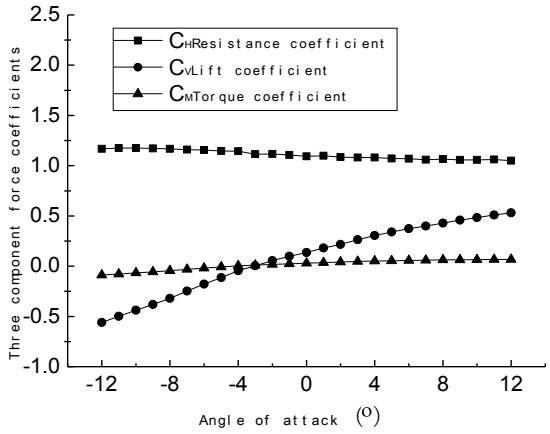

Figure 9 Curves of Three Component Force Coefficients of Baling River Bridge

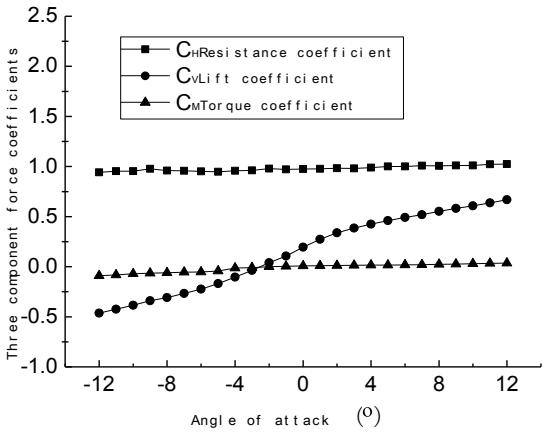

Figure 10 Curves of Three Component Force Coefficients of Dimu River Bridge

3.2 Dynamic Response

In order to simulate the elastic restraint between test section and other main beam section, the model of dynamic test is suspended by four string in the wind tunnel. Spring coefficient is determined by the similar conditions. Tests can be used to find flutter critical wind speed under different attack angle and verify vortex-induced vibration and galloping if applicable. The tests can also determine the wind speed, the amplitude of vibration and strouhal number of the main beam when vortex-induced vibration happens. Thus flutter and vortex-induced vibration performance of the main beam can be evaluated.

Tests are carried out under smooth oncoming flow, figure 11 and figure 12. The damping ratio is assumed to be 0.5% relative to the critical. Considering the adverse wind flow in the gorge, five attack

angles, 0°,+3°,-3°,+6° and -6°, were carried out. No vortex-induced vibration in vertical and torsional direction of the two bridges was observed. The flutter wind speed two bridges are listed in Table 2. It can be seen in the Table 2 that when the attack angle of the incoming flow is -3°, the flutter critical wind speed of Baling River Bridge is less than flutter checking wind speed. The amount of surplus with 0° attack angle is very small, so the main beam section need to do optimization test. When the attack angle of the incoming flow is 0°, -3° or -6°, the flutter critical wind speed of Dimu River Bridge are larger than flutter checking wind speed. But when the attack angle of the incoming flow is +3° or +6°, the flutter critical wind speed of Dimu River Bridge are less than flutter checking wind speed. Then they don't meet the requirements of bridge design. So main beam of both two bridges need to do aerodynamic optimization test.

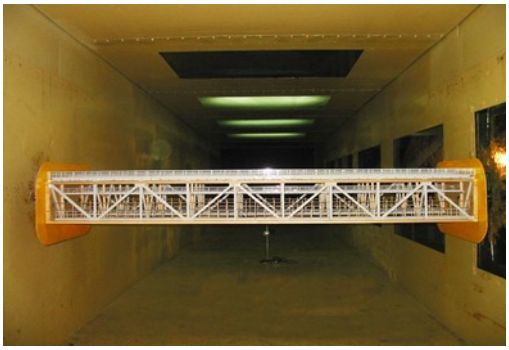

Figure 11 Section Model of Baling River Bridge

Figure 12 Section Model of Dimu River Bridge

Table2 Flutter Critical Wind Speed of the Two Bridges

Baling River Bridge				Dimu River Bridge			
Attack angle	Flutter Critical Wind Speed /(m·s^{-1})	Flutter checking Wind Speed /(m·s^{-1})	Safety evaluation	Attack angle	Flutter Critical Wind Speed /(m·s^{-1})	Flutter checking Wind Speed /(m·s^{-1})	Safety evaluation
-6°	51.3		Safe	-6°	>64		Safe
-3°	38.8		Unsafe	-3°	>64		Safe
0°	43.7	41.3	Safe	0°	>64	57.6	Safe
+3°	71.2		Safe	+3°	53		Unsafe
+6°	48.6		Safe	+6°	50		Unsafe

4 Aerodynamic Optimization Test on Main Deck

Basis on the results of section model tests, when the attack angle of the incoming flow is -3°, the flutter critical wind speed of Baling River Bridge is less than flutter checking wind speed. The amount of surplus with 0° attack angle is very small, so the main beam section need to be tested optimization test. When the attack angle of the incoming flow is +3° or +6°, the flutter critical wind speed of Dimu River Bridge are less than flutter checking wind speed. In order to make the bridges meet the design requirements, and avoid bridges destructed by flutter, wind tunnel test is needed to do a serious of aerodynamic optimization test studies on main beam of the two bridges.

4.1 Baling River Bridge

For Baling River Bridge, this paper have tested two types of tests, single wing plate and double wing plate section model test. Flutter test has been tested after the groove of the deck is sealed, the results of it have been compared with the results come from tests that when unsealed groove and aerodynamic wing plate work together. Double wing plate are supported by upright columns, which is made of ABS plate, that beside the maintaining roadway. The section of it is ellipse with long axis of 23.3 mm and short axis of 2.5 mm. (Figure 12 and Figure 13). The results from the tests when unsealed groove and double aerodynamic wing plate have worked together are in Table 3.

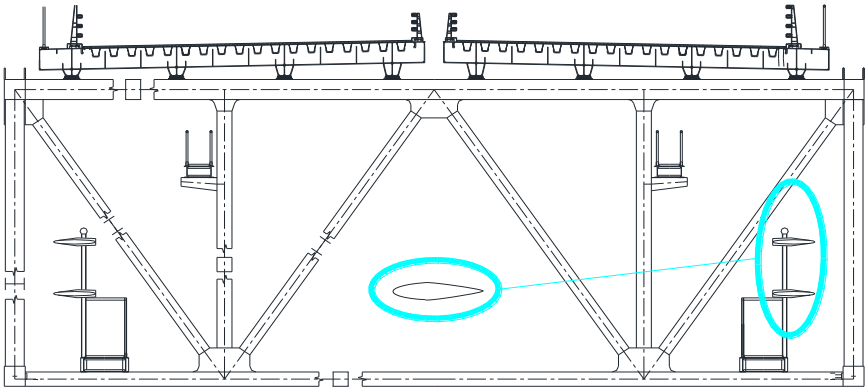

Figure 12 Truss Beam Section with Double Wing Plate

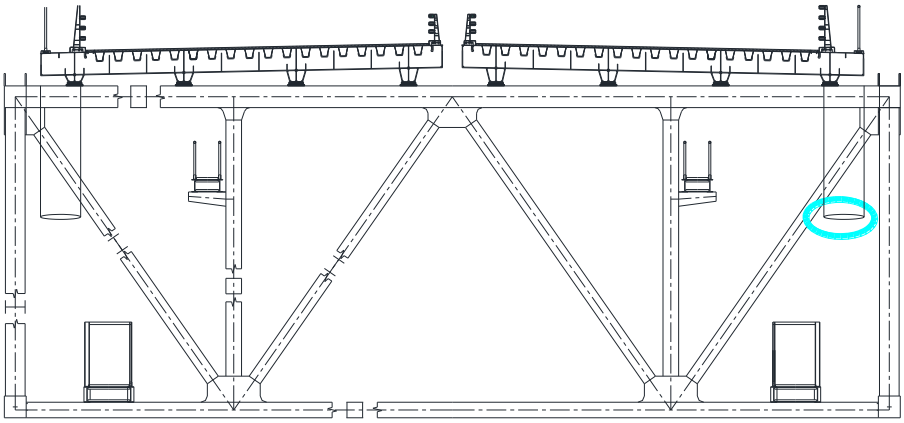

Figure 13 Truss Beam Section with Single Wing Plate

Table 3 Flutter Divergence Wind Speed
When Unsealed Groove and Double Aerodynamic Wing Plate Have Worked Together

Anti-vibration Measures	Attack angle (°)	Flutter Divergence Wind Speed /(m·s^{-1})	Measures	Attack angle (°)	Flutter Divergence Wind Speed /(m·s^{-1})
Double wing plate and the groove is 10mm	-3	>107.7	Double wing plate and the groove is sealed	-3	81.3
Double wing plate and the groove is 10mm	0	>107.7	Double wing plate and the groove is sealed	0	67.6
Double wing plate and the groove is 10mm	+3	56.3	Double wing plate and the groove is sealed	+3	49.9
the groove is 10mm	-3	>102.8	the groove is sealed	-3	75.9

the groove is 10mm	0	72.5	the groove is sealed	0	51.4
the groove is 10mm	+3	53.9	the groove is sealed	+3	45.5

Based on a serious of section model tests, different types of aerodynamic wing plate that are installed on the deck and have obviously different characteristics to affect flutter stability. Aerodynamic wing plate have obvious positive impact on flutter stability, but it can be significantly affected by wind attack angle and the number of plates. Single wing plate in proper position can increase flutter critical wind speed by 15%. If wind attack angle is 0°, double wing plate have a better function. The highest flutter critical wind speed can be increased by 48%. The location that the wind plate installed can affect flutter critical wind speed.

4.2 Dimu River Bridge

For selecting the best program, the worst effects wind attack angle, which is +6°, is been chosen to do aerodynamic optimization test. The optimization programs and results of the main beam are listed in table 4. The data in the table are converted to actual data that of actual bridge not of model.

Table 4 Aerodynamic Optimization Programs

Anti-vibration Measures	Graphic	Program	Flutter Divergence Wind Speed /(m·s^{-1})
Install horizontal deflector	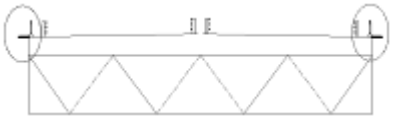	Program 1 the width of horizontal deflector is 1.5 m	52
Seal the groove of main beam	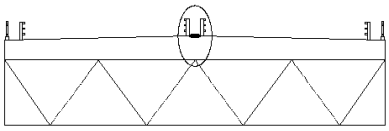	Program 2	52
Seal the groove of main beam and install central stabilized plate above the deck	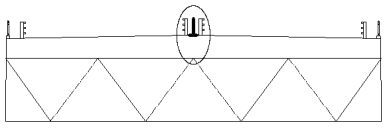	Program 3 the height of central stabilized plate is 0.55 m Program 4 the height of central stabilized plate is 1.10 m	54 57
Seal the groove of main beam and install central stabilized plate below the deck	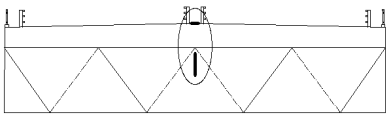	Program 5 the height of central stabilized plate is 1.0. m Program 6 the height of central stabilized plate is 1.50 m Program 7 the height of central stabilized plate is 1.75 m Program 8 the height of central stabilized plate is 2.00 m	53 55 63 63
Use grille seal the groove	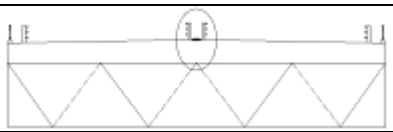	Program 9 Ventilation rate of the grille is 50%	53
Use grille seal the groove and install central stabilized plate below the deck	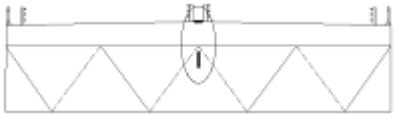	Program 10 Ventilation rate of the grille is 25% and the height of central stabilized plate is 1.00 m Program 11 Ventilation rate of the grille is 50% and the height of central stabilized plate is 1.00 m Program 12 Ventilation rate of the grille is 50% and the height of central stabilized	55 56 58

	plate is 1.00 m, which are installed at intervals.	
Program 13	Ventilation rate of the grille is 50% and the height of central stabilized plate is 1.00 m, which are installed at intervals, and the upper edge of stabilized plate close to surface of main truss beam)	64

As table 4 shows, based on a serious optimization section model tests. All programs have certain effects on increasing flutter critical wind speed, but the effects are different. The differences are as follows.

Installing horizontal deflector, or sealing the groove, or using grille to seal the groove, every method can only increase flutter critical wind speed by 2-3 m/s. They practically don't improve the aerodynamic performance of main beam. And the horizontal deflector has a bad effect on the appearance of the bridge.

Sealing the groove completely and installing central stabilized plate with the height of 0.55 m or 1 m above the deck, they can increase flutter critical wind speed, and the higher the central stabilized plate, the higher the flutter critical wind speed. But all flutter critical wind speed in these condition are less than flutter checking wind speed. And the central stabilized plate also has a bad effect on the appearance of the bridge.

Sealing the groove completely and installing central stabilized plate with the height of 1 m, 1.5m, 1.75 m or 2 m below the deck, they all can increase flutter critical wind speed. When the height of central stabilized plate is less than 1.75m, the flutter critical wind speed increases with the central stabilized plate's height. But when the height of central stabilized plate is more than 1.75m, the flutter critical wind speed doesn't increase any more. Therefore, if using the method that seal the groove completely and install central stabilized plate below the deck to increase flutter critical wind speed, the highest of central stabilized plate should be 1.75 m, and now the flutter critical wind speed is 63 m/s. But if the central stabilized plate is high, it will waste material and increase difficulties to installation.

Using grille seal the groove and installing central stabilized plate with the height of 1m above the deck at intervals. Through several programs, when the ventilation rate of the grille is 50%, the grille is discontinuously arranged and the upper edge of plate close to surface of main beam, the flutter critical wind speed is 64 m/s. This program save materials, such as grille and central stabilized plate, and reduce the wind load of main beam. And the height of central stabilized plate is reduced to 1 m. It is convenient for installation.

Based on the above analysis, this paper recommend that for Dimu River Bridge the following optimization measures are adopted, which is using grille with ventilation rate in 50% seal the groove of the beam and installing central stabilized plate at intervals, which is disconnected at the crossbeam, and its upper edge close to the surface of main beam (Figure 9 and Figure 10).

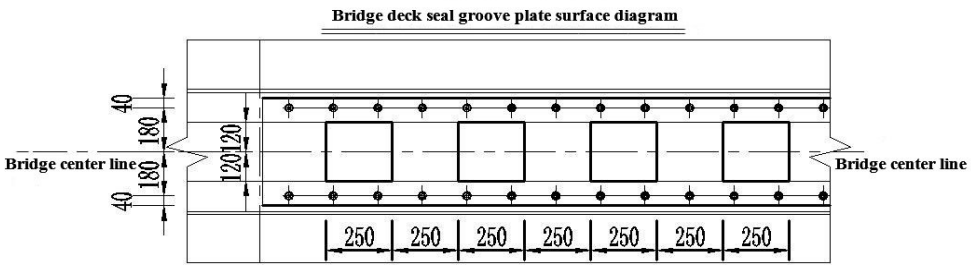

Figure 9 Use Grille Seal the Groove of Main Beam of Dimu River Bridge

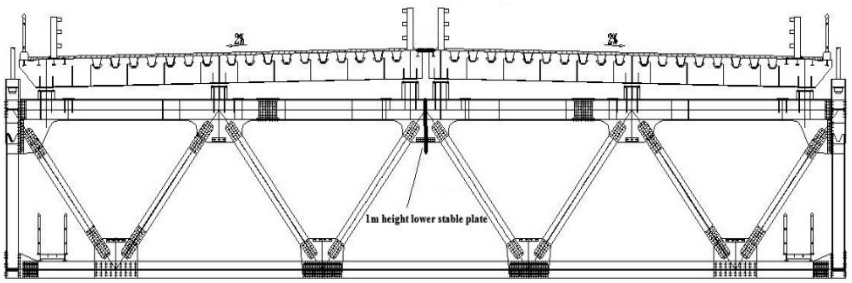

Figure 10 Center Stabilized Plate of Dimu River Bridge

5 Conclusions

Based on studies on the selection of wind parameters, section model test and anti-vibration measures of Baling River Bridge and Dimu River Bridge. This paper have got the following conclusions.

In the gorge of mountain area, the average wind speed can be obvious amplified, and in different gorge wind speed and the amplification are different. Every gorge has its own characteristic.

For different truss beam, even if the width of main beams are same, the aerodynamic characteristics are different. And this paper recommend the aerodynamic forces of truss girder should be obtained by wind tunnel tests

For long-span suspension bridges that are constructed in the mountain areas, flutter instability is a key factor in bridge design. The flutter instability of main beam is low when wind attack angle of incoming flow is positive, then the main beam usually needs aerodynamic shape optimization.

Installing aerodynamic wing plate or central stabilized plate can help to increase flutter critical wind speed. The location, continuity and height of aerodynamic wing plate and central stabilized plate have a great impact on flutter critical wind speed.

References

Wang Kai, et al. 2013. Determination method for basic design wind speed of mountainous valley bridge[J]. *Journal of Southwest Jiaotong University*, 48(1): 29-36.

Scanlan, R.H. 1978. The action of flexible bridges under wind, I: flutter theory. *Sound Vib*, 60(2),187-199.

Agar, T. J. A. 1989. Aerodynamic flutter analysis of suspension bridges by a modal technique. *Eng.Struct*, 11(2),75-82.

Beith J.G. 1998. A practical engineering method for the flutter analysis of long-span bridges. *Wind.Eng.Ind.Aerodyn*, 77-78,357-366.

Chen, Z. Q. Agar T. J. 1994. Finite element-based flutter analysis of cable-suspended bridges (discussion), *Struc.Eng,* ASCE, 120(3),1044-1046.

Tanaka H. Yamamura N. Tatsumi M. 1992. Coupled mode flutter analysis using flutter derivatives. *Wind Eng.Ind.Aerodyn*, 42(1-3),1279-1290.

Katsuchi ,H. Jones N. P. ,Scanlan R. H. 1999. Coupled flutter and buffeting analysis of the Akashi-Kaikyo Bridge. *Struct.Eng*.,ASCE, 125(1),60-70.

Miyata T.Yamada H. 1990. Coupled flutter estimate of a suspension bridge. *Wind. Eng.Ind. Aerodyn*, 33(1-2),341-348.

Dung N. N. Miyata T. Yamada H. Minh N. N. 1998. Flutter responses in long span bridges with wind induced displacement by the mode tracing method. *Wind. Eng.Ind. Aerodyn*. 77-78,367-379.

Ge Y. J. Tanaka H. 2000. Aerodynamic flutter analysis of cable-supported bridges by multi- mode and full-mode approaches. *Wind.Eng.Ind.Aerodyn*, 86(2-3), 123- 153.

Scanlan R. H. 2000. Motion-related body-force functions in two-dimensional low-speed flow. *Fluids Strcut*., 14(1),49-63.

Bucher C. G. Lin Y .K. 1988. Effect of span wise correlation of turbulence field on the motion stochastic stability of long-span bridges. *Fluids and Structures*, 2(5), 437-451.

Lin Y. K. Li Q. C. 1993. New stochastic theory for bridge stability in turbulent flow. *Eng. Mech*., 119(1),113-128.

Chen X.. Matsumoto M. Kareem A. 2000. Time domain flutter and buffeting response analysis of bridges. *Eng.Mech.*,ASCE, 126(1),7-16.

Scanlan R H Tomko J. 1971. Airfoil and bridge deck flutter derivatives. *Journal of Engineering Mechanics*. ASCE, 97(6):1717-1237

Xu Hongtao, Liao Haili, Li Mingshui. 2009. Wind tunnel test study of sectional model of baling river bridge[J]. *World Bridges*, 37(4): 83-89.

Scanlan R H, Tomko J J. 1971. Airfoil and Bridge Deck Flutter *Derivatives*.ASCE. 97(6):1717-1737

Xu Fuyou, Chen Airong, Zhang Zhe. 2008. Practical technique for determ ining critical flutterw ind speed of bridgemodel. *Journal of Vibration and Shock,* 27(12): 97-102.

Chen Zhengqing, OuYang Kejian, Niu Huawei. 2009. Aerodynamic mechanism of improvement of flutter stabil ity of truss-girder suspension bridge using central stabil izer. *China Journal of Highway and Transport*, 22(6):53-59.

Zhu L D, Wang M, Wang D L. 2007. Flutter and buffeting performances of third Nanjing bridge over Yangtze river under yaw wind via aeroelastic model test [J]. *Journal of Wind Engineering and Industrial Aerodynamics*, 95(9-11): 1579-1606.